Crystal Structure Refinement of the Layered Copper–Titanium Perovskites $Ln_2Ba_2Cu_2Ti_2O_{11}$ (Ln = La, Nd) from Neutron Powder Diffraction Data

Pedro Gómez-Romero,* María Rosa Palacín, and Juan Rodríguez-Carvajal†

Institut de Ciència de Materials de Barcelona (CSIC), Campus de la U.A.B. 08193, Bellaterra, Barcelona, Spain

Received June 1, 1994. Revised Manuscript Received August 1, 1994®

Neutron powder diffraction data of the oxides $Ln_2Ba_2Cu_2Ti_2O_{11}$ (Ln = La, Nd) are presented and analyzed by means of Rietveld profile refinements. These data confirm the existence, in both cases, of a tetragonal superstructure based on a quadruple perovskite ($a_p \times a_p \times 4a_p$). Whereas the Nd derivative presents complete long range order of Cu/Ti, Ln/Ba, and oxygen vacancies, in the lanthanum derivative this order is only partial.

Introduction

Recent efforts in the field of layered copper perovskites have led to the discovery of a new class of structure with oxygen vacancies ordered in planes leading to an $a_p \times a_p \times 4a_p$ superstructure (where a_p would be the parameter of a typical cubic perovskite cell). The first example of such a quadruple perovskite was a mixed copper–tin oxide of formula $La_2Ba_2Cu_2Sn_2O_{11}$.[1] More recently, independent work by Gormezano and Weller and our own group on Cu–Ti perovskites has led to the isolation of the related oxides $Gd_2Ba_2Cu_2Ti_2O_{11}$[2] and $Ln_2Ba_2Cu_2Ti_2O_{11}$ (Ln = La, Nd, Eu).[3-5]

Our study of this new family of oxides $Ln_2Ba_2Cu_2Ti_2O_{11}$ (Ln = La, Nd, Eu) forms part of our research in mixed perovskites of copper and other transition metals[3,6] and has included X-ray and electron diffraction, magnetic susceptibility measurements, and chemical and thermogravimetric analyses. The latter confirmed the oxygen contents, whereas X-ray powder diffraction patterns and electron diffraction patterns indicated a structure of the perovskite type with a tetragonal distortion and a fourfold superstructure along c.[3,5] Those preliminary studies already showed varying degrees of order of the cations and oxygen vacancies as well as an increase of the tetragonal distortion in going from the La to the Eu derivative.

Despite the consistent set of data and the reasonable results obtained from the profile analysis of the X-ray diffraction pattern of the europium derivative, a neutron diffraction study was necessary to obtain more reliable information on the location of oxygen vacancies and on the possible order of cations. Copper and titanium for instance have very different scattering lengths (0.7718 and −0.3438 respectively), whereas their X-ray scattering powers are similar enough to prevent an unambiguous determination of their distribution by choosing among different ordering schemes.[3,6] The same is true for Ln and Ba ions. Furthermore, our results and those reported by Weller et al.[2] were mostly coincident but differed in key points concerning the possibility of the synthesis and the structure of the lanthanum derivative; a claim that layered $La_2Ba_2Cu_2Ti_2O_{11}$ could not be synthesized was made by these authors. This made necessary further structural studies by neutron diffraction.

We report here two neutron profile refinements of the compounds $La_2Ba_2Cu_2Ti_2O_{11}$ and $Nd_2Ba_2Cu_2Ti_2O_{11}$ in order to complete the structural characterization of these phases. The europium derivative could not be studied due to its excessive absorption cross section for neutrons.

Experimental Section

The synthesis of the title compounds has been reported previously in detail[3,5] and made use of the ceramic method. Thus, Ln_2O_3 (Ln = La, Nd), $BaCO_3$, CuO, and TiO_2 (all >99.9% purity) were used. La_2O_3 was treated at 1000 °C for 15 h prior to use to ensure its purity; the other compounds were used without further purification. Stoichiometric amounts of those reactants (calculated to yield ca. 1 g of product) were thoroughly ground and mixed together. The mixture was heated in alumina crucible (Alsint) at a rate of 100 °C h^{-1} up to 900 °C and kept at that temperature for 2 h to allow for the decomposition of the carbonate; then it was further heated (100 °C h^{-1}) to 1100 °C for 24 h, and was finally cooled to room temperature also at a rate of 100 °C h^{-1}. This cycle was followed by the diffractometric analysis of the product, and the second step (treatment at 1100 °C) repeated until the X-ray diffraction pattern was unchanged from one cycle to the next. This took typically two cycles.

Neutron powder diffraction experiments were carried out at room temperature on the Orphee reactor of the Laboratoire Leon Brillouin (CEA-CNRS, Centre d'Etudes de Saclay). The diffractometer D1A-G4.2 was used for this work. This dif-

* To whom correspondence should be addressed.
† Laboratoire Léon Brillouin (CEA-CNRS), Centre d'Etudes de Saclay, 91191 Gif sur Yvette Cedex, France. On leave from Institute Laue-Langevin, 156 X, 38042 Grenoble, France.

® Abstract published in *Advance ACS Abstracts,* September 15, 1994.

(1) Anderson, M. T.; Poeppelmeier, K. R.; Zhang, J.-P.; Fan, H.-J.; Marks, L. D. *Chem. Mater.* **1992**, *4*, 1305–13.
(2) Gormezano, A.; Weller, M. T. *J. Mater. Chem.* **1993**, *3*, 771–2.
(3) Palacín, M. R. Masters Thesis, Universitat Autonoma de Barcelona, Spain, 1993.
(4) Palacín, M. R.; Fuertes, A.; Casañ-Pastor, N.; Gómez-Romero, P.. Presented at the IV Reunion Nacional de Materiales, 19–21 Oct **1993**, Oviedo, Spain.
(5) Palacín, M. R.; Fuertes, A.; Casañ-Pastor, N.; Gómez-Romero, P. *Adv. Mater.* **1994**, *6*(1), 54–7.
(6) Palacín, M. R.; Bassas, J.; Rodriguez-Carvajal, J.; Gomez-Romero, P. *J. Mater. Chem.* **1993**, *3*, 1171–7.

0897-4756/94/2806-2118$04.50/0

fractometer was installed in the cold neutron guide G4 during the refurbishment of the reactor of the Institut Laue-Langevin. The wavelength used had an approximate value of 2.58 Å. The primary neutron beam comes from the reflection (004) of a small flat Ge monochromator at a takeoff angle of $2\theta_M = 134°$. Due to the particular spectrum of the neutron guide the contamination with the $\lambda/2$ harmonics is lower than 0.15% in integrated intensity; therefore, the corresponding peaks have been neglected in the refinements. The diffractometer is constituted by a bank of ten detectors that moves to cover a whole angular range of 160° in 2θ. Each detector is equipped with a soller collimator of 10 min of arc. A program that combines the spectrum recorded by each detector, making efficiency and relative position of detectors corrections, provides a full profile affected with the proper coefficients to calculate the standard deviations of each observed averaged counts per step. The step size used in the experiments was 0.10° (2θ). The available Q range ($Q = 4\pi \sin\theta/\lambda$) was 0.21–4.79 Å^{-1}; therefore, the crystal structures that can be refined should be of moderate complexity, as is the present case. The fine details of the structure (specially temperature factors) cannot be determined with enough accuracy for the diffractometer configuration used. Profile refinements, using the Rietveld method, were carried out with the help of program FULLPROF.[7] Used scattering lengths (in units of 10^{-12} cm) were La 0.8240; Nd 0.7690; Ba 0.5070; Cu 0.7718; Ti −0.3438; O 0.5803.

Results and Discussion

Our previous X-ray and electron diffraction studies on these oxides[3,5] have shown in all cases a superstructure corresponding to a cell $a_p \times a_p \times 4a_p$. This superstructure, associated with a tetragonal distortion and with space group *P4/mmm*, is best detected from electron diffraction studies, but it is also apparent from powder X-ray diffraction patterns of the samples with a larger tetragonal distortion (Nd and Eu derivatives). The X-ray diffraction pattern of the La derivative shows no split peaks, but its electron diffraction pattern presents weak but significant superstructure spots.[3,5]

In addition to this major superstructure, a minor one is also detected from electron diffraction data, but only in the cases of Nd and Eu. This implies a redefinition of the unit cell to $\sqrt{2}a_p \times \sqrt{2}a_p \times 8a_p$ with a corresponding change to space group *I4/mmm*. This minor superstructure was not detected in the case of La, which presents at most an $a_p \times a_p \times 4a_p$ cell (*P4/mmm*) with weaker superstructure spots that in the cases of Nd or Eu.

Neutron powder diffraction patterns for $La_2Ba_2Cu_2Ti_2O_{11}$ and $Nd_2Ba_2Cu_2Ti_2O_{11}$ are shown in Figures 1a,b respectively. Despite the clear differences between them, in principle both can be indexed in space group *P4/mmm*, corresponding to the symmetry detected by X-ray diffraction. Even though the superstructure peaks corresponding to the tetragonal distortion of these perovskites are weaker in the neutron diffraction pattern of the lanthanum derivative, they are clearly present and prevent a cubic indexation of its pattern. The differences between the structures of both oxides can be better understood from the individual profile refinements described below.

Profile Refinement for $La_2Ba_2Cu_2Ti_2O_{11}$. First of all, we carried out refinements of the neutron diffraction data for this oxide in space group *Pm3m* to check for the possibility of total disorder in the perovskite structure. Whereas the main strong peaks could be adequately indexed with this cubic symmetry, the model failed to account for several weak but significant superstructure peaks, most evident at low angles. Furthermore, a refinement in space group Pnma, corresponding to a disordered model with a $GdFeO_3$-type distortion, such as that found for the related three-dimensional oxide La_2CuTiO_6, was also inadequate. Space group *P4/mmm* was subsequently used in all refinements of this structure. The starting structural model was analogous to that found from an X-ray profile analysis made on the related Eu derivative.[3,5] After several initial cycles to optimize global profile parameters, atomic positions and temperature factors, the refinement of site occupancies already showed the presence of a substantial degree of disorder, including the nonnegligible occupancy factor of an oxygen atom at (0,0,0).

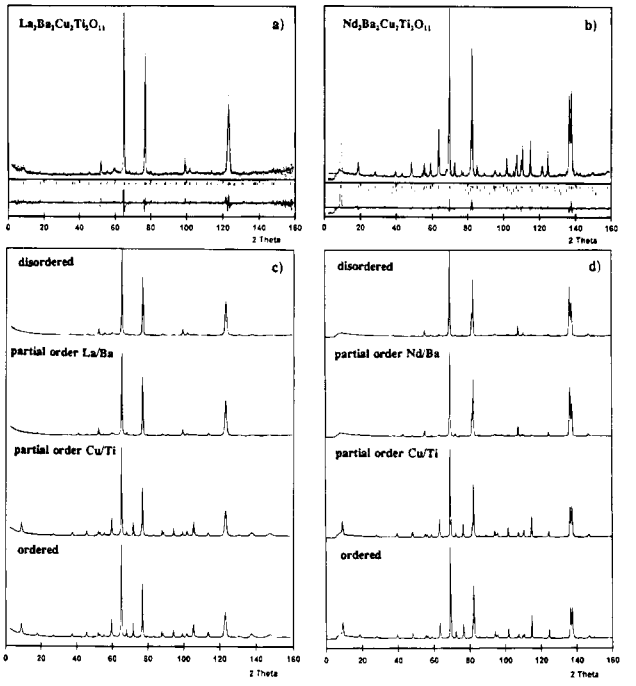

Figure 1. (a) Experimental neutron diffraction pattern for $La_2Ba_2Cu_2Ti_2O_{11}$ (dots) and results of the profile refinement: calculated pattern (continuous line); difference $y_{obs} - y_{calc}$ (bottom line) and allowed Bragg reflections (vertical bars). (b) Experimental neutron diffraction pattern for $Nd_2Ba_2Cu_2Ti_2O_{11}$ (dots) and results of the profile refinement: (as in Figure 1a). Peak 001 is shown but was not included in the refinement for difficulties to account properly for its background. (c) Calculated profiles for idealized models accounting for the indicated degrees of order in $La_2Ba_2Cu_2Ti_2O_{11}$ (realistic background, peak width etc used in the simulations). (d) Same as in (b) for the oxide $Nd_2Ba_2Cu_2Ti_2O_{11}$ (positional and thermal parameters used were those from $La_2Ba_2Cu_2Ti_2O_{11}$).

To get an idea of the effect of order/disorder on the neutron diffraction pattern of the tetragonally distorted structure under study, we carried out profile calculations incorporating realistic profile parameters such as background and peak widths, using four possible models: (i) total disorder between La/Ba, Cu/Ti, and O(0,0,1/2)/O(0,0,0); (ii) partial order of only La/Ba pair; (iii) partial order of only Cu/Ti and O(0,0,1/2)/O(0,0,0); (iv) perfect order of all three pairs. Figure 1c shows all these calculated diffraction patterns. Significant differences can be observed, especially for the low angle peaks. Interestingly, the intensity of peak (0,0,1) seems

(7) J. Rodríguez-Carvajal, Program FULLPROF (Version 2.5, April 1994, ILL, unpublished).

Table 1. Final Results for Each of the Refined Models (See Text)

model[a]	description		R_p[b]	R_{wp}	R_{exp}	χ^2	a (Å)	c (Å)
	$La_2Ba_2Cu_2Ti_2O_{11}$							
L1	P4/*mmm*		10.07	13.0	6.79	3.70	3.9367(3)	15.805(2)
	$Nd_2Ba_2Cu_2Ti_2O_{11}$							
N1	*P4/mmm* x(Ti) = 0	x(O4) = 0	4.28	5.33	2.60	4.21	3.91275(6)	15.7614(3)
N2	*P4/mmm* x(Ti) = y(Ti) = 0.076	x(O4) = 0	4.21	5.19	2.59	4.01	3.91275(6)	15.7614(3)
N3	*P4/mmm* x(Ti) = 0.103	x(O4) = 0.006	4.21	5.19	2.59	4.01	3.91275(6)	15.7614(3)
N4	*P4/mmm* x(Ti) = 0.103	x(O2) = 0.009	4.20	5.19	2.59	4.01	3.91275(5)	15.7614(3)

[a] Models N2, N3, and N4 were identical to N1 (Table 3) except for the indicated coordinates. [b] $R_p = 100\ (\sum_i|y_i - yc_i|)/(\sum_i|y_i|)$; $R_{wp} = 100\ [(\sum_i w|y_i - yc_i|^2)/(\sum_i w|y_i|^2)]^{1/2}$. $R_{expected} = 100[(N - P + C)/(\sum_i w|y_i|^2)]^{1/2}$; the goodness of fit: $\chi^2 = [R_{wp}/R_{expected}]^2$ where $N - P + C$ is the number of degrees of freedom (N is the number of points in the pattern, P the number of refined parameters, and C the number of constraint functions).

Table 2. Final Atomic Parameters for $La_2Ba_2Cu_2Ti_2O_{11}$

atom	domain[a]	x	y	z	B (Å^2)	occupancy[b]
La1	1	0.5000	0.5000	0.0000	1.3(3)	0.64(1)
Ba1′	1′	0.5000	0.5000	0.5000	1.3(3)	0.36(1)
Ba2	1	0.5000	0.5000	0.2329(14)	1.3(3)	1.28(1)
La2′	1′	0.5000	0.5000	0.7329(14)	1.3(3)	0.72(1)
La3	1	0.5000	0.5000	0.5000	1.3(3)	0.64(1)
Ba3′	1′	0.5000	0.5000	0.0000	1.3(3)	0.36(1)
Cu1	1	0.0000	0.0000	0.113(4)	3.4(6)	1.28(1)
Cu1′	1′	0.0000	0.0000	0.613(4)	3.4(6)	0.72(1)
Ti2	1	0.0000	0.0000	0.387(9)	3.4(6)	1.28(1)
Ti2′	1′	0.0000	0.0000	0.887(9)	3.4(6)	0.72(1)
O1	1	0.0000	0.0000	0.5000	3.0(2)	0.64(1)
O1′	1′	0.0000	0.0000	0.0000	3.0(2)	0.36(1)
O2	1	0.5000	0.0000	0.3716(13)	3.0(2)	2.55(1)
O2′	1′	0.5000	0.0000	0.8716(13)	3.0(2)	1.45(1)
O3	1	0.0000	0.0000	0.2688(16)	3.0(2)	1.28(1)
O3′	1′	0.0000	0.0000	0.7688(16)	3.0(2)	0.72(1)
O4	1	0.5000	0.0000	0.1039(15)	3.0(2)	2.55(1)
O4′	1′	0.5000	0.0000	0.6039(15)	3.0(2)	1.45(1)

[a] Coordinates of atoms in domain 1′ are obtained by adding vector (0,0,0.5) to those of atoms in domain 1. [b] In units of atoms per unit cell. Set to add up to a total stoichiometry $La_2Ba_2Cu_2Ti_2O_{11}$, with relative values within each domain according to each site multiplicity and with both domains adding to 100%. Numbers in parentheses are estimated standard deviation on the least significant figures for the refined parameters.

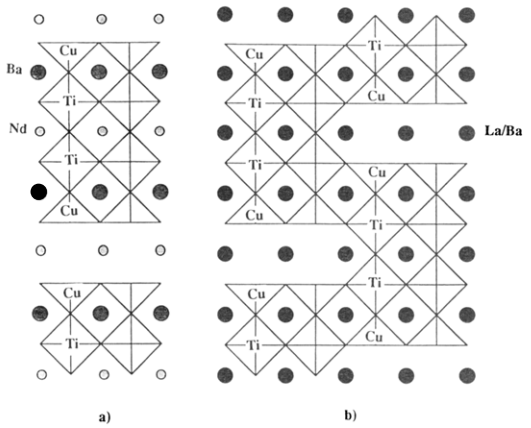

Figure 2. (a) Schematic diagram of the structure for $Nd_2Ba_2Cu_2Ti_2O_{11}$ where the ordered arrangement of cations and oxygen vacancies extend to long range. (b) Scheme of the structural model proposed to explain the partial order found in $La_2Ba_2Cu_2Ti_2O_{11}$. Here two ordered domains, displaced by $(0,0,^1/_2)$ with respect to each other are shown. La and Ba were also found to be subject to a partial statistical disorder (see text).

associated to the order of Cu/Ti, while that of peak (0,0,2) is mostly associated to La/Ba order. This is not unexpected since vectors between equivalent metals in both Cu/Ti and La/Ba sublattices correspond exactly to the crystallographic spacings of the corresponding peaks. When we look at the experimental diffraction pattern, both peaks (0,0,1) and (0,0,2) present intensities somewhere in between the cases of total order and disorder, thus confirming the presence of partial, imperfect long range order within the tetragonal structure of $La_2Ba_2Cu_2Ti_2O_{11}$.

Finally, a quantitative refinement of the structural model was performed in order to obtain further structural details. In the final stages of refinement it would be normal to refine occupancy factors while fixing the corresponding thermal parameters. We followed this procedure, but the values thus obtained were not too reliable: our results showed some refined occupancy factors like those of Cu and Ti that made chemical sense, but others, like the occupancies of La and Ba among the three possible sites of the structure result in values which do not add exactly to the expected 1:1 ratio between La and Ba. The final result appeared satisfactory according to the reliability factors, but the structural model obtained was not chemically reasonable. Consequently, our final approach avoided the refinement of many independent occupancy factors and consisted of the refinement of a single parameter describing the relative "abundance" of two ordered microdomains with the same crystal structure but displaced origins. The spacially disordered and local nature of the origin displacement allows the treatment of this kind of disorder simply by putting the displaced atoms in the asymmetric unit of a single phase. In such a model the occupancies of each atom within a domain are tied up according to the ideal occupancies of each atom in an ordered arrangement as found for the Eu derivative.[5] Furthermore, the relative abundances of both domains are constrained to add to 100%, and thus only one parameter of disorder is refined. Among the several structural models tried with this approach, the best results corresponded to a model were the coordinates of atoms in one domain had been shifted by half a unit cell along c, with respect to those in the other domain, with an additional redefinition of the positions of La and Ba to introduce partial disorder of these ions (see Table 2). Figure 2b schematizes this model, the origin shift and the crystallographic relation between the proposed domains. This way relative abundances of the domains were 64% and 36%, far from a 50:50 mixture which would come closest to total disorder. Table 1 includes the final reliability factors obtained for this compound. Final atomic parameters and occupancies for all atoms are given in Table 2. Selected bond distances and angles within a single domain are given in Table 4. Overall, the coordination geometries seem reasonable, i.e., a Jahn–Teller elongated square-pyramidal coordination for Cu and a compressed axial Ti–O bond; nevertheless we must note that the existence of partial disorder, accounted for by the micro-

domain model,[8] could introduce some additional uncertainty in the refined values beyond the given statistical standard deviations.

Profile Refinement for $Nd_2Ba_2Cu_2Ti_2O_{11}$. Comparison of the experimental diffraction pattern (Figure 1b) with the calculated patterns based on the several degrees of order (Figure 1d) shows already a closest resemblance to an ordered model. A Rietveld refinement was performed to obtain fine structural features. As before, the starting structural model in space group *P4/mmm* was based on the results of the previous X-ray profile refinement for the Eu derivative. In addition to the main phase, small amounts of reaction intermediates ($BaTiO_3$ and Nd_2CuO_4) were detected and accounted for in the refinements (Figure 1b) by inclusion of their known crystal structure in the calculation of the profile.

After several refinements with a gradual increase in the number of parameters, including fractional coordinates, the overall starting model (Figure 2a) seemed to be confirmed. Oxygen stoichiometry and vacancy ordering were confirmed by refinement of the corresponding occupancy factors. Thus, a hypothetical oxygen atom located at the origin, which would have completed octahedral coordination for all B ions in the structure, got a refined occupancy of −0.002(1). On the other hand, all the remaining oxygens ended up with slightly overstoichiometric factors upon refinement and confirmed their full occupancy.

We also carried out refinements to detect cation ordering. As an example, considering partial occupation of site Nd1 both by Nd and Ba and refining their occupancies (constrained to add to 1) while keeping their thermal factors identical and constant led to occupancy values (atoms/unit cell) of 1.08(4) for Nd and −0.08(4) for Ba. Similar results were obtained for site Nd2, while site Ba3 refined to a slightly understoichiometric occupancy for barium.

Refinement of Cu and Ti occupancies (while keeping their thermal parameters identical and fixed) led to the following values in atoms per unit cell: square-pyramidal sites, Cu, 1.94(4) Ti, 0.06(4); octahedral sites, Ti, 1.73(1), Cu, 0.27(1). The total amounts of Cu (2.21) and Ti (1.79), which should add to two in each case, show the uncertainty in these refinements. In this case, this deficiency seems associated mainly with the octahedral metal site occupancy since a parallel anomaly in the refinement of its thermal parameter also occurs; Cu and Ti would therefore be ordered within experimental error according to these refinements. Occupancy factors were accordingly fixed to the corresponding stoichiometric values in the final stages of refinement.

With respect to the space group used for these refinements we want to point out that, in addition to the major superstructure observed by X-ray and electron diffraction on these oxides, a minor superstructure corresponding to a cell $\sqrt{2}a_p \times \sqrt{2}a_p \times 8a_p$ was also deduced for the Nd and Eu derivatives by electron diffraction.[3,5] This larger unit cell, with its probably associated orthorhombic symmetry would therefore be the strictly correct description of our lattice; nevertheless, neither the X-ray nor the present neutron diffraction patterns are able to detect that minor superstructure. This must be due to a combination of the very different volumes of sample irradiated in electron diffraction as compared with X-ray or neutrons plus the greater difference in the intensities of superstructure and main reflections in the later cases. Under these circumstances refining with the larger cell would only introduce more refined parameters with a low chance of reaching a meaningful minimum upon refinement. Indeed, several refinements conducted in space group *I4/mmm* with the larger unit cell led to chemically unreasonable results with only a minor improvement in the values of reliability factors, but no apparent difference in the profile refined. This is the reason why we have kept the smaller *P4/mmm* cell for the present refinements. In addition we must also note that many of the very weak peaks observed in the diffraction pattern which cannot be indexed with this tetragonal cell are accounted for not by considering the larger superstructure either but only by assigning them to unreacted intermediates of the reaction as we have finally done.

Table 3. Final Atomic Parameters for $Nd_2Ba_2Cu_2Ti_2O_{11}$ (Model N1)[a]

atom	x	y	z	B (Å^2)	occupancy[b]
Nd1	0.5000	0.5000	0.0000	1.07(13)	1.00000
Ba2	0.5000	0.5000	0.2357(3)	1.58(15)	2.00000
Nd3	0.5000	0.5000	0.5000	1.86(14)	1.00000
Cu1	0.0000	0.0000	0.1084(2)	3.12(9)	2.00000
Ti2	0.0000	0.0000	0.3701(7)	6.7(4)	2.00000
O1	0.0000	0.0000	0.5000	5.9(2)	1.00000
O2	0.5000	0.0000	0.3841(2)	4.30(9)	4.00000
O3	0.0000	0.0000	0.2554(3)	3.49(10)	2.00000
O4	0.5000	0.0000	0.0974(2)	2.23(8)	4.00000

[a] In model 2, x(Ti) = y(Ti) refined to 0.076(4); in model 3, x(Ti) refined to 0.103(5) and x(O4) to 0.006(13) while the rest of the atomic coordinates were the same within experimental error. [b] In atoms per unit cell. Numbers in parentheses are estimated standard deviation on the least significant figures for the refined parameters.

The results of the final refinement are given in Table 1, atomic parameters are summarized on Table 3, and selected bond distances and angles for this refined structure (model N1) are given on Table 4.

The final parameters agree well with those obtained from the X-ray profile refinement of the europium derivative, and the result unambiguously shows the existence of order both for the Ln–Ba and Cu–Ti cations and for the oxygen vacancies. The only unusual result is the large thermal parameter obtained for titanium. We believe that this could be caused by a local rhombic distortion of the Ti position and its coordination sphere which could not be properly accounted for with the imposed tetragonal symmetry. This fine structural feature could only be reliably obtained from neutron data using a shorter wavelength. In fact we have tried an alternative refinement considering a slight displacement of Ti away from its *4mm* site into a disordered fourfold set with x(Ti) = y(Ti) (model N2); this alternative increases the number of refined parameters and certainly leads to a reduced, more reasonable thermal parameter for Ti (1.3(6) Å^2) which would end up in a strongly distorted O_h site. The final reliability factors improve somewhat, but the result can be hardly taken as a preferable final solution, especially in view of the similar reliability factors obtained between this model and model N3, where the displacement of Ti is re-

(8) A reviewer of this work has pointed out the possibility of clustering of the oxygen vacancies in this case, which might be only approximately described by the microdomain model proposed here.

Table 4. Selected Bond Distances (Å) and Angles (degrees)[a]

$La_2Ba_2Cu_2Ti_2O_{11}$		$Nd_2Ba_2Cu_2Ti_2O_{11}$ model N1	
La1–O4	8 × 2.563(15)	Nd1–O4	8 × 2.487(1)
Ba2–O2	4 × 2.95(2)	Ba2–O2	4 × 3.049(4)
Ba2–O3	4 × 2.841(7)	Ba2–O3	4 × 2.7841(7)
Ba2–O4	4 × 2.83(2)	Ba2–O4	4 × 2.929(4)
La3–O1	4 × 2.7837(2)	Nd3–O1	4 × 2.7667(1)
La3–O2	8 × 2.827(15)	Nd3–O2	8 × 2.677(2)
Cu1–O3	2.47(7)	Cu1–O3	2.317(6)
Cu1–O4	4 × 1.973(5)	Cu1–O4	4 × 1.9640(3)
Ti2–O1	1.78(15)	Ti2–O1	2.047(11)
Ti2–O2	4 × 1.984(19)	Ti2–O2	4 × 1.9688(13)
Ti2–O3	1.88(15)	Ti2–O3	1.808(12)
O3–Cu1–O4	4 × 94(2)	O3–Cu1–O4	4 × 95.1(2)
O4–Cu1–O4	2 × 172(3)	O4–Cu1–O4	2 × 169.87(15)
O4–Cu1–O4	4 × 89.7(2)	O4–Cu1–O4	4 × 89.554(13)
Cu1–O4–Cu1	172(3)	Cu1–O4–Cu1	169.87(15)
O1–Ti2–O2	4 × 97(5)	O1–Ti2–O2	4 × 83.6(3)
O1–Ti2–O3	180	O1–Ti2–O3	180
O2–Ti2–O2	2 × 165(6)	O2–Ti2–O2	2 × 167.1(5)
O2–Ti2–O2	4 × 89.1(8)	O2–Ti2–O2	4 × 89.28(5)
O2–Ti2–O3	4 × 83(4)	O2–Ti2–O3	4 × 96.4(4)

[a] Numbers in parentheses are estimated standard deviations on the least significant figures.

strained along a (Table 1). The rhombic coordination of Ti must be taken at this time as a hypothetical explanation which in any case is not so relevant to the central problem of the order–disorder of cations and oxygen vacancies.

Another possible statistical disorder that we have analyzed deals with the positions of oxygen atoms in the structure. In the related Sn–Cu quadruple perovskite, a displacement of equatorial oxygens (O2 and O4) from their ideal position has been proposed[1] to occur to minimize the mismatch between alternating Cu and Sn layers. Furthermore, this displacement could account for a minor superstructure present in the Cu–Sn compound, similar, though not identical, to the minor superstructure we have detected in the Cu–Ti systems. We have therefore tried refining models with statistically disordered oxygen atoms. Models N3 and N4 introduce this posibility; in addition to the titanium disorder the following parameters were obtained: x(O4) refined to 0.006(13) (Model N3), x(O2) refined to 0.009(15), thus representing a negligible rotation of copper and titanium coordination polyhedra respectively. Obviously the refinement is not sensitive to this kind of oxygen disorder, as can be seen from Table 1. On the other hand, the titanium disorder seems to improve the refinement but leads to chemically dubious results.[9] Thus, in our case, some kind of Ti distortion, rather than oxygen rotation is qualitatively detected and could be taken in principle as a possible origin of the minor superstructure. Unfortunately the characteristics of neutron diffraction as compared with electron diffraction, as mentioned above, prevent the manifestation in the diffraction pattern of peaks from the superstructure and thus make a quantitative evaluation impossible and prevent the unambiguous assignment of a structural feature to that superstructure.

Conclusions

Neutron diffraction studies have confirmed the existence of order among the different cations and oxygen vacancies forming the structure of the title oxides. This order is only partial, or not extended to long range in the case of the La derivative, which nevertheless presents a clear superstructure with a tetragonal unit cell. A possible description of its structure as a cubic perovskite is ruled out. In the case of the Nd derivative and, by extension, for other smaller lanthanides like Eu, the order is most apparent and implies the segregation in planes of oxygen vacancies with a concomitant ordering of Cu/Ti and Ln/Ba pairs occupying preferentially square-pyramidal sites with a typical Janh–Teller distortion (Cu), octahedral sites (Ti), cubic and regular cuboctahedral sites (Ln), and larger cuboctahedral sites (Ba).

Acknowledgment. We thank the Spanish DGICYT (PB93-0122), CICYT (MAT93-0240-C04-01), and the MIDAS Program (93-2331) for financial support, and the Generalitat de Catalunya for a predoctoral fellowship to M.R.P.

(9) In model N2 for instance, the following bond distances resulted: Ti–O1 2.046(13); 2 × Ti–O2 2.009(6); Ti–O2 2.38(3); Ti–O2 1.55(3); Ti–O3 1.904(15); corresponding to an unreasonably large axial distortion. Similar results were obtained for model N4.